Published in final edited form as:
Neurotox Res. 2013 November ; 24(4): 549–559. doi:10.1007/s12640-013-9410-7.

Role of PGE_2 EP1 receptor in intracerebral hemorrhage induced brain injury

Nilendra Singh[1,*], **Bo Ma**[2,*], **Christopher Charles Leonardo**[1], **Abdullah Shafique Ahmad**[1], **Shuh Narumiya**[3], and **Sylvain Doré**[1,4]

[1]Department of Anesthesiology, Center for Translational Research in Neurodegenerative Disease, University of Florida, Gainesville, 32610, FL, USA

[2]Neurogenetics Division, National Institute on Aging, Bethesda, 21225, MD, USA

[3]Department of Pharmacology, Kyoto University, Kyoto 606-8315, Japan

[4]Departments of Neuroscience, Neurology, and Psychiatry, University of Florida, Gainesville, 32610 FL, USA

Abstract

Prostaglandin E_2 (PGE_2) has been described to exert beneficial and detrimental effects in various neurologic disorders. These conflicting roles of PGE_2 could be attributed to its diverse receptor subtypes, EP1-EP4. At present, the precise role of EP1 in intracerebral hemorrhage (ICH) is unknown. Therefore, to elucidate its possible role in ICH, intrastriatal injection of collagenase was given in randomized groups of adult male wildtype (WT) and EP1 receptor knockout ($EP1^{-/-}$) C57BL/6 mice. Functional outcomes including neurologic deficits, rotarod performance, open field activity, and adhesive removal performance were evaluated at 24, 48 and 72 h post ICH. Lesion volume, cell survival, and death, were assessed using Cresyl Violet, and Fluoro-Jade staining, respectively. Microglial activation and phagocytosis were estimated using Iba1 immunoreactivity and fluorescently-labeled microspheres. Following 72 h post ICH, $EP1^{-/-}$ mice showed deteriorated outcomes compared to the WT control mice. These outcomes were demonstrated by elevated neurological deficits, exacerbated lesion volume, and significantly worsened sensorimotor functions. Fluoro-Jade staining showed significantly increased numbers of degenerating neurons and reduced neuronal survival in $EP1^{-/-}$ compared to WT mice. To assess *in-vivo* phagocytosis, the number of microspheres phagocytosed by Iba1-positive cells was 145.4±15.4% greater in WT compared to $EP1^{-/-}$mice. These data demonstrate that EP1 deletion exacerbates neuro-behavioral impairments following ICH, potentially by slowing down/impairing microglial phagocytosis. A better understanding of this EP1 mechanism could lead to improved intervention strategies for hemorrhagic stroke.

Keywords

Collagenase; Hematoma; Microglia; Neurodegeneration; Prostaglandin

Corresponding author: Sylvain Doré PhD, Center for Translational Research in Neurodegenerative Disease, University of Florida, 1275 Center Drive, Biomed Sci J493, PO Box 100159, Gainesville, FL 32610-0159. Phone: 352-273-9663; Cell: 443-803-1910; Fax: 352-294-5060; sdore@ufl.edu.
*Both authors contributed equally.

Introduction

Spontaneous intracerebral hemorrhage (ICH) is the deadliest and most debilitating form of stroke with a first year mortality rate as high as 50% to 60% (Qureshi et al. 2001; Ribo and Grotta 2006; Go et al. 2013). ICH forms a parenchymal hematoma that triggers mechanical and irreversible primary brain damage and is characterized by shearing and damage of the blood vessel, neurons, axons and blood brain barrier (Aronowski and Zhao 2011; Keep et al. 2012). Within hours to days after hemorrhage, extravasated blood and its components are released, causing secondary brain injury. These events trigger inflammation, excitotoxicity, oxidative stress, and cell death, which subsequently lead to severe functional deficits (Wang and Doré 2007b). Contrary to primary damage, secondary damage is preventable and treatable with intervention at the appropriate time after insult (Wang and Doré 2007b; Aronowski and Zhao 2011; Keep et al. 2012). Microglia becomes activated within minutes after injury to offset secondary damage (Xue and Del Bigio 2000; Aronowski and Hall 2005). These resident immune cells migrate to the lesion site, where they engulf blood products and damaged/dead tissue to promote repair within the brain parenchyma (Giulian et al. 1989; Zhao et al. 2007; Smirkin et al. 2010). Removal of tissue debris facilitates endogenous repair, in part, by upregulating neurotrophic factors (Tang et al. 2010; James et al. 2010; Yang et al. 2008) and potentially by inhibiting pro-inflammatory cytokine signaling (Huynh et al. 2002; Hoffmann et al. 2005). Thus, these observations support the *in vivo* clearance of degenerating tissue as a therapeutic target for ICH.

Prostaglandin E_2 plays an important role in the initiation and maintenance of both normal and pathological responses to brain injury (Ahmad et al. 2008; Doré et al. 2003; Phillis et al. 2006; Ahmad et al. 2013). PGE_2 is formed from arachidonic acid by cyclooxygenase and PGE_2 synthase enzymes, and binds to the heteromeric G-protein coupled receptors E-prostanoid (EP) 1, 2, 3 and 4. Since EP receptors have differential effects on intracellular calcium levels, phosphotidylinositol turnover and cyclic adenosine monophosphate (cAMP) production, a better understanding of prostaglandin pathways may uncover additional therapeutic strategies.

Previous reports from our lab and others showed that EP1 deletion prevents neurotoxicity in both excitotoxic and focal ischemic models (Ahmad et al. 2006; Kawano et al. 2006). Additionally, pharmacological inhibition of EP1 improves anatomical and functional outcomes in excitotoxicity, oxygen glucose deprivation, and ischemic stroke models (Ahmad et al. 2006; Ahmad et al. 2008; Zhou et al. 2008). Moreover, genetic deletion of EP1 significantly improved CBF at reperfusion and increased neuronal survival after transient focal ischemia in mice (Saleem et al. 2007). EP1 activation leads to PLC-dependent Ca^{2+} release and PKC activity, which have also been shown to mediate microglial phagocytosis (Hebert et al. 1990; Funk et al. 1993; Abe et al. 2013; Watabe et al. 1993). Several studies have implicated COX/prostaglandin signaling in the pathologic progression of ischemic stroke (Doré et al. 2003; Choi et al. 2006). However, to the best of our knowledge, the role of EP1 in ICH remains unknown.

Based upon these observations, the present study was conducted to determine the neuro-behavioral outcomes in wildtype (WT) and EP1 receptor knockout ($EP1^{-/-}$) mice subjected to collagenase-induced ICH, and to investigate whether microglial activation mediates these effects. For these purposes, WT and $EP1^{-/-}$ mice were subjected to ICH for subsequent examination of anatomical and neuro-behavioral outcomes at selected time points after ICH injury.

Materials and Methods

Mice

All procedures were approved by the Institutional Animal Care and Use Committee at the University of Florida. Adult male WT and EP1$^{-/-}$ C57BL/6 mice of 11–13 weeks old (24–28 g) were bred and maintained in our animal facilities. The EP1$^{-/-}$ mice grow normally and have no gross abnormalities in behavior and brain macroscopic vasculature anatomy indices when compared to WT mice (Saleem et al. 2007). Mice were given food, water ad libitum and housed under controlled reverse light cycle conditions (23±2°C; 12 h light/dark cycle).

Collagenase-induced ICH model

Age- and weight-matched male mice were anesthetized with isoflurane (3% initial, 1% to 1.5% maintenance) and immobilized on a stereotaxic frame. A small incision was made at overlying skin over the skull and a single unilateral intrastriatal injection of collagenase VII-S [0.04 Units (U) in 0.2 μl saline, Sigma] was given at the following stereotactic coordinates relative to bregma: 0.5 mm anterior, 2.4 mm lateral, 3.2 mm from dura in WT and EP1$^{-/-}$ mice. (Wang et al. 2006; Clark et al. 1998). Rectal temperature was monitored and maintained at 37.0°C±0.5°C throughout the surgical and recovery periods. Mice were allowed to survive up to 72 h after ICH injury.

Functional assessments

Various functional outcomes were tested in WT and EP1$^{-/-}$ mice following ICH by an experimenter blinded to the experimental cohorts. Wherever necessary each group received pre-training for three consecutive days before surgery followed by neuro-behavioral testing at 24, 48 and 72 h after ICH injury. All the neuro-behavioral and functional tasks were done at the same time of the day and in between each task 30–45 m of rest was given to mice.

Neurological deficit scoring—It was assessed 72 h post hemorrhagic injury using the 24-point scale (Clark et al. 1998). The tests included body symmetry, gait, climbing, circling behavior, front limb symmetry, and compulsory circling. Each test was graded from 0 to 4, establishing a maximum deficit score of 24.

Open field locomotor activity—Automated MED Associates (St. Albans, VT) open field activity monitor was used with video tracking interface system. This test is a sensitive method of measuring both gross and fine locomotor activity and values are given as ambulatory and stereotypic counts. The activities were assessed 24 h before the induction of hemorrhage and 24, 48, and 72 h post ICH. Briefly, mice were individually housed in four transparent acrylic cages and their simultaneous activities were recorded over a 30-m test period. The results are expressed as total ambulatory and stereotypic counts for each mouse for test period.

Adhesive removal test—This test is an indicator of the somatosensory dysfunction following ICH in mice (Komotar et al. 2007; Schallert et al. 2000). Briefly, mice were trained for this test for three successive days before ICH. The mouse is removed from the home cage and small circular adhesive tape (Teeny Tough Spots-USA Scientific; Ocala, FL) with a diameter of 4.7 mm is placed on the distal radial region of the left or right forelimb paw. The time (in seconds) taken to contact and remove the sticky tape for each forelimb is recorded. Maximum time allowed to remove the tape was set at 120 s.

Rotarod test—Rotarod Rotamex 5 machine and software (Columbus, OH) were used to measure the mice equilibrium and motor deficits following brain injury (Dunham and Miya

1957; Jones and Roberts 1968). Briefly, mice were trained and tested on accelerating speed rotarod; starting speed was kept at 5 rpm and its maximum accelerating speed was 50 rpm. All mice were pre-trained repeatedly for three days before surgery and at 24, 48, 72 h post-surgery. The total run time was collected automatically by Rotamex computer software.

Histology and immunohistochemistry

Following 24 or 72 h after ICH mice were deeply anesthetized and transcardially perfused with phosphate-buffered saline (PBS, pH 7.4) followed by fixation with 4% paraformaldehyde. The brains were quickly harvested and processed for histology and immunohistochemistry using Leica CM 1850 cryostat. The mounted sections were stained with Cresyl Violet to estimate the lesion volume (Ahmad et al. 2006). Fluoro-Jade B (Histo-Chem, Inc. Jefferson, AR) was used as a neuronal degeneration marker (Schmued and Hopkins 2000; Wasserman and Schlichter 2007) and semi-quantitative analysis was performed. For fluorescent immunohistochemistry, free-floating sections were rinsed in PBS containing 0.1% Triton X-100 (PBST) and incubated for 1 h at room temperature in 5% goat serum (Sigma, St. Louis, MO) to block nonspecific binding. All primary antibodies were diluted in PBST and applied overnight at 4°C. After being rinsed in PBST the sections were incubated for 2 h with the secondary antibody, which was conjugated with Alexa-488, Cy2, or Cy3 (1:1000; Jackson Labs). After being rinsed again all sections were mounted in DAPI Hardest Reagent (Vector Labs.) under a glass coverslip. Antibody concentrations used for immunohistochemistry were: rabbit anti-Iba1 (1:1000; Wako), and rat anti-Ter119 (1:500; Santa Cruz). To further assess the location of EP1 receptor, double immunofluorescence was carried out with primary rabbit anti-EP1 polyclonal antibody (1:500; Cayman) in combination with rat anti-CD11b (1:1000; Serotec), mouse anti-NeuN (1:250; Chemicon), or rat anti-GFAP (1:200; Zymed). After being rinsed in PBST the sections were incubated for 2 h with the appropriate secondary antibody. To use as negative controls, additional sections were incubated without the primary antibodies. Stained sections were examined with a Nikon TE2000-E Eclipse fluorescence microscope (Nikon Instruments Inc.). The images were captured and analyzed by SPOT advanced image software (Diagnostic Instruments Inc.). To quantify the numbers of positive cells, four images from the region of interest from each section were randomly acquired.

β-galactosidase activity

To measure β-galactosidase activity, free-floating sections were rinsed in PBS containing 0.1% Triton X-100 (PBST) and stained with a solution of 5 mg/mL X-gal, 2 mM $MgCl_2$, 50 mM $K_3Fe(CN)_6$, and 50 mM $K_4Fe(CN)_6$ in PBS overnight at 37°C. Sections were counterstained with nuclear fast red (Simmer et al. 2009).

In vivo phagocytosis assay

The *in vivo* phagocytosis assay was adapted from an established protocol (Koizumi et al. 2007). Briefly, two hours after the induction of the intracerebral bleeding, 1 μl of fluorescently-labeled microspheres (red, 1 μm diameter, 0.025%, Sigma) were injected into the same site. Free-floating sections of 12 μm containing the microsphere-injected sites were thoroughly washed in PBST (by shaking 10 times for 10 m each) to remove the nonspecific binding of the microspheres and were stained with rabbit polyclonal anti-Iba1 antibody (green) to visualize microglia. The microspheres in the four regions of interest were counted and the average was used as an index of *in vivo* phagocytosis. Three sections covering the entire hematoma were analyzed per animal and four animals were used in each group for analysis of *in vivo* phagocytosis.

Statistics

The statistical comparisons were made by one- and two-way (in multiple groups) ANOVA, followed by Bonferroni post hoc analysis. The differences between two groups were determined by an unpaired two-tailed Student's t test, except for neurologic deficit scores, which were calculated by the non-parametric Mann Whitney test. Data are expressed as mean±SD. GraphPad Prism 5 software was used for statistical analysis. In all comparisons, a *P* value less than 0.05 was considered to be significant.

Results

Mortality

Initially, 0.05 U of collagenase was used to induce ICH and we found that the mortality rate in WT was 30%; however, EP1$^{-/-}$ mice had a significantly higher mortality rate of 90%. In subsequent experiments, 0.04 U yielded approximately 10% mortality rate in WT and 30% in EP1$^{-/-}$ mice, and was able to produce reproducible lesions and functional deficits in both genotypes. The experimental model resulted in a non-significant reduction in body weight in both groups.

EP1 receptor deletion deteriorates functional and neurological outcomes after ICH

To assess the role of EP1 on neuro-behavioral and functional outcomes after ICH, WT and EP1$^{-/-}$ mice were subjected to hemorrhagic injury and tested before and 24, 48 and 72 h after ICH for neurological deficit scores, locomotor activity in open field, adhesive removal task, and accelerating rotarod performance. Behavioral testing was performed by an experimenter blinded to the genotypes.

Neurological Deficit Score—At 72 h after ICH, EP1$^{-/-}$ mice showed significantly higher deficits compared to WT mice (6.7±1.3 vs. 12.0±2.4; $P<0.0001$; n=6; Fig. 1A).

Accelerating rotarod performance task—During training, both genotypes exhibited improved performance for three consecutive days with no significant differences. At 24 h after ICH, both genotypes showed significant reductions in time on rotarod compared with pre-surgery times (WT: 90.5±18.8 vs. 20.0±25.5 s; EP1$^{-/-}$: 100.5±25.5 vs. 15.4±25.1 s; $P<0.001$). At 72 h after ICH, WT mice showed significant improvements compared to EP1$^{-/-}$ mice (54.7±18.7 vs. 16.6±10.5; $P<0.05$; n=6; Fig. 1B).

Adhesive removal test—During training, both WT and EP1$^{-/-}$ mice removed the tape from both forepaws in approximately 10–15 s by day 3 compared to day 1 (Left forepaw: WT: 11.0±4.5 vs. 48.5±8.4 s; EP1$^{-/-}$: 12.5±3.1 vs. 54.6±9.3 s and Right forepaw: WT: 6.2±1.7 vs. 29.0±5.2 s; EP1$^{-/-}$: 7.2±1.8 vs. 28.5±9.3 s; Fig. 1C, D). At 24 h post-ICH, WT and EP1$^{-/-}$ mice showed significant impairments in removal times, as most mice were unable to remove the tape within the allotted 120 s. Further, both WT and EP1$^{-/-}$ mice showed improved somatosensory function by 72 h post-ICH (Left forepaw: WT: 51.6±10.5 s, EP1$^{-/-}$: 87.6±6.0 s; Right forepaw: WT: 19.3±4.9 s; EP1$^{-/-}$: 68.0±18.2 s). However, WT mice recovered faster compared to EP1$^{-/-}$ mice ($P<0.05$). Interestingly, our findings suggest that both WT and EP1$^{-/-}$ mice spend less time removing adhesive tape from their right forepaws (WT: 6.2±1.7 s; EP1$^{-/-}$: 7.2±1.8 s) compared to their left forepaws (WT: 11.6±4.5 s; EP1$^{-/-}$: 12.5±3.1 s; Fig. 1C and D), and recovery is faster with the right forepaw compared to the left forepaw.

Open field test—Stereotypic movements significantly declined at 24 h after ICH in WT (1220.9±186.6 vs. 1748.9±287.2 counts) and EP1$^{-/-}$ mice (760.5±176.2 vs. 1706.7±415.7

counts). Upon comparison, $EP1^{-/-}$ exhibited poor performance compared to WT mice (760.5±176.2 vs. 1220.9±186.6 counts; $P<0.05$; n=6). At 72 h post-ICH, stereotypic movements improved in both groups and were restored to baseline levels in WT. However, $EP1^{-/-}$ had significantly fewer movements as compared to WT (1119.7±381.9 vs. 1836.9±203.0 counts; Fig. 1E). Similarly, ambulatory distance was significantly reduced in WT (1048.3±299.7 vs. 458.1±277.8 counts) and $EP1^{-/-}$ mice (1128.0±222.7 vs. 398.8±332.9 counts) at 24 h after ICH, and WT mice performed better than $EP1^{-/-}$ (1357.7±263.1 vs. 708.6±353.8 counts; $P<0.05$; n=6; Fig. 1F) at 72 h post-ICH.

EP1 receptor deletion aggravates brain injury

Intracerebral collagenase injection produces consistent intrastriatal hematoma, as evident from Cresyl Violet staining (Fig. 2A). Quantification showed that lesion volume was 52.8% smaller in WT compared to $EP1^{-/-}$ mice (7.5±4.3 vs. 14.2±2.6 mm^3, $P<0.01$; n=6) at 72 h post-ICH.

EP1 receptor deletion exacerbates neuronal cell death

To assess secondary injury following ICH, brain sections were stained with Fluoro-Jade B, a marker of degenerating neurons. Quantification of the peri-hematoma region showed more degenerating neurons in $EP1^{-/-}$ (110.5±17.4 cells/field; n=4) compared to WT mice (68.7±9.7 cells/field; $P<0.02$; n=4; Fig. 2B). No Fluoro-Jade B staining was observed in the contralateral hemisphere or sham group, but in some instances it was observed along the needle track. In CV stained sections, surviving neurons were also quantified around the hematoma region. $EP1^{-/-}$ mice showed significant reductions in surviving neurons relative to WT mice at 72 h post-ICH ($P<0.001$; n=4; Fig 2C).

EP1 receptor is expressed in activated microglia

To determine the cellular location of EP1 receptors, X-gal staining was performed in conjunction with double immunofluorescence for distinct cell surface markers. X-gal staining showed that β-galactosidase was mainly expressed in the peri-hematoma region in $EP1^{-/-}$ mice at 72 h, whereas WT mice showed weak signal (Fig. 3A). Furthermore, EP1 receptor immunoreactivity was associated with activated microglia (Fig. 3B), while we were unable to detect co-immunoreactivity of EP1 receptor with neurons or astrocytes.

EP1 receptor contributes to microglial activation

Microglia present in the peri-hematoma regions following IHC exhibited round amoeboid phenotypes, cell bodies more than 10 μm in diameter and short, thick processes, consistent with the activated, phagocytic state (Ito et al. 2001). Cells were labeled with the microglia/macrophage cell surface marker Iba1 and the activation profile was evaluated based upon these criteria. The number of activated microglia was markedly increased in WT mice from 24 to 72 h after ICH, whereas cell numbers in $EP1^{-/-}$ markedly decreased during the same time frame. Quantification analysis further shows that the numbers of activated microglia in WT mice increased significantly to 61.3 ± 4.3% at 24 h and to 344.9 ± 24.4% at 72 h as compared with $EP1^{-/-}$ after ICH ($P<0.001$ for 24 and 72 h; n=4; Fig. 3C).

Phagocytosis is down regulated by EP1 receptor deletion

Immunopositive remnants of red blood cells were engulfed by activated microglia in the peri-lesion regions (Fig. 4A). To quantify microglial phagocytosis *in vivo,* fluorescently-labeled microspheres were injected into the lesion site after ICH. Microsphere incorporation into microglia was confirmed with Iba1 immunofluorescence. Activated, Iba1-positive cells displaying short, thick processes accumulated in peri-hematoma regions and appeared to colocalize with microsphere-derived fluorescent signal (Fig. 4B). Quantification showed that

significantly fewer microspheres were incorporated into Iba1-positive cells in $EP1^{-/-}$ mice relative to WT mice at 72 h post-ICH ($P<0.001$; n=4; Fig. 4C). Interestingly, injection of microspheres after ICH caused mortality in $EP1^{-/-}$ mice.

Discussion

The present study showed that PGE_2 EP1 receptor deletion augments collagenase-induced ICH injury in mice, causing severe neurological and functional deficits. $EP1^{-/-}$ mice showed more pronounced neurodegeneration after ICH compared to WT. Data also demonstrated EP1 expression by Iba1-positive immune cells and an apparent EP1 requirement for these cells to incorporate microspheres. Taken together, these findings show for the first time that EP1 deletion exacerbates ICH injury and slows hematoma resolution, potentially by inhibiting microglial phagocytosis. Thus, selective EP1 modulation has therapeutic potential in preventing/minimizing ICH injury.

Several experimental models are used to recapitulate ICH injury, each with strengths and limitations (MacLellan et al. 2008). We used intrastriatal injection of collagenase type VII S. Exogenous collagenase application reproduces spontaneous and stable hemorrhage and re-bleeding over time by causing multiple ruptures in blood vessels, resulting in hematoma expansion and edema (Wu et al. 2006; MacLellan et al. 2008). Previous reports showed substantial hematoma volume following intrastriatal collagenase injection (Chen et al. 2011; Gu et al. 2009), and *in vitro* data showed that typical collagenase concentrations used for ICH do not cause direct neuronal cell death or inflammation (Chu et al. 2004; Matsushita et al. 2000). In the present study, a drastic increase in mortality of $EP1^{-/-}$ mice after injection of 0.05 U collagenase led us to decrease the dose to 0.04 U, thus reducing $EP1^{-/-}$ mortality while producing stable and reproducible hematomas in both genotypes. Importantly, $EP1^{-/-}$ mice consistently exhibited greater hemorrhagic injury compared to WT, suggesting a protective role for EP1.

Clinical studies have shown that hemorrhage volume is an early indicator of neurological and functional outcomes (Davis and Donnan 2006; Broderick et al. 1999). Here, we used four different neuro-behavioral tests with high sensitivity for detecting deficits after ICH. Our lab and others have used neurological deficit scoring successfully in ICH injury (Clark et al. 1998; Shah et al. 2011). The present study demonstrated impaired outcomes in $EP1^{-/-}$ mice relative to WT that were also extended to more complex sensorimotor functions. Behavioral pretesting showed significant improvements throughout the training period irrespective of genotype, indicating that EP1 deletion does not impair learning and memory retention. However, WT mice performed significantly better than $EP1^{-/-}$ from 24 h to 72 h post-ICH, reflecting differences due to ICH. Additionally, we measured hemoglobin content within injured tissue to clarify whether EP1 deletion affects the original bleeding volume induced by collagenase. No significant differences were detected between WT and $EP1^{-/-}$. Previous findings suggested that the breakdown/lysis of red blood cells contributes to secondary injury (Wang et al. 2007; Keep et al. 2012; Aronowski and Zhao 2011). These lysed RBCs release free heme, hemoglobin, and iron within or around the hematoma, contributing to irreversible neuronal damage and death (Zhao et al. 2007; MacLellan et al. 2008; Keep et al. 2005; Regan and Panter 1993; Wang et al. 2007). Indeed, intracerebral infusion of collagenase causes rapid cell death in mice, which is in accord with other findings in mice, rats and pigs (Wasserman and Schlichter 2007; Gu et al. 2009; Wang and Doré 2007a). Here, tissue damage mainly occurred proximal to the hematoma, and the increased cell death/reduced neuronal survival observed in $EP1^{-/-}$ suggests a potential role for EP1 in regulating toxicity associated with lysed RBC byproducts.

Genetic deletion and/or pharmacological blockade of EP1 receptor attenuates brain injury and improves neurological outcomes in NMDA-induced excitotoxicity and ischemic models (Ahmad et al. 2008; Ahmad et al. 2006; Saleem et al. 2007; Abe et al. 2009). In apparent contrast with those findings, we found that EP1 deletion exacerbates brain injury and deteriorates functional outcomes following ICH. This shows a dynamic role of EP1 activation that may depend upon specific neural sequelae, and the present study implicates microglial activation in mediating responses unique to ICH. The beneficial or detrimental effects of microglial activation remain controversial (Nguyen and Benveniste 2002; Zhao et al. 2009; Keep et al. 2005). For example, attenuation of brain microglial activation has been shown to confer protection in various models of neurodegeneration (Yrjanheikki et al. 1999; Tikka and Koistinaho 2001), whereas growing evidence suggests a protective role for activated microglia in CNS pathologies, including brain hemorrhage (Giulian et al. 1989; Zhao et al. 2007). Interestingly, we found EP1 receptors were present around the hematoma and appeared to co-localize with the microglial marker Iba1. Moreover, WT mice displayed increased microglial activation compared to $EP1^{-/-}$. Because microglia play reparative roles within the CNS, particularly concerning phagocytosis following tissue damage, it is conceivable that genetic or pharmacologic inhibition of microglial function might delay recovery.

To determine whether impaired phagocytic capacity might account for exacerbated injury in $EP1^{-/-}$, we used fluorescent microsphere beads (Koizumi et al. 2007). Data showed a significantly higher number of Iba1-positive cells that incorporated microsphere beads in WT mice compared with $EP1^{-/-}$, suggesting a role in phagocytosis and clearance of cellular debris. If phagocytosis accounts for ICH protection, this raises important implications for potential treatment strategies. Although a role for EP1 in mediating this effect is provocative, more studies are needed to confirm these results. Since the precise signaling pathways are unknown, several other possibilities exist, including phagocytic microglial receptors metabotropic P2Y6 receptor and TREM2 receptor which have been reported recently (Koizumi et al. 2007; Takahashi et al. 2005). Based on initial findings, we speculate that microglial TREM2-mediated phagocytosis would play an essential function for brain homeostasis (Takahashi et al. 2007). Activation of the P2Y6 receptor or TREM2 signaling in microglia triggers phagocytosis through the pathway(s) mediated by PLC-linked Ca^{2+} and PKC. EP1 activation also leads to a PLC-dependent Ca^{2+} release and PKC activity (Funk et al. 1993; Hebert et al. 1990; Watabe et al. 1993). It has been also suggested that of the PGE_2 receptors, EP1 and EP3 are involved in PGE_2-mediated cell migration (Carlson et al. 2009; Cimino et al. 2008), suggesting that EP1 may facilitate the migratory response of microglia after brain injury.

Conclusions

In conclusion, we found that genetic deletion of EP1 augments hemorrhagic brain injury, with significant deterioration in functional and neurological deficits. This enhanced brain injury leads to more cell death and reduced cell survival in the $EP1^{-/-}$ mice compared to their respective WT controls. Moreover, these data suggest that EP1 is expressed by microglia and EP1 deletion dampens microglial activity and phagocytosis. Altogether, our findings reinforce the unique role of EP1 in ICH, suggest a mechanism through microglial phagocytosis, and support EP1 targeting as a novel pharmacological approach to improve hemorrhagic stroke outcomes.

Acknowledgments

Financial support: We thank all Doré lab team members for their active participation. National Institutes of Health (NS046400, AG022971) to SD, and the American Heart Association (09POST2080364) to BM.

References

Abe S, Watabe H, Takaseki S, Aihara M, Yoshitomi T. The effects of prostaglandin analogues on intracellular Ca2+ in ciliary arteries of wild-type and prostanoid receptor-deficient mice. J Ocul Pharmacol Ther. 2013; 29 (1):55–60.10.1089/jop.2011.0197 [PubMed: 23046436]

Abe T, Kunz A, Shimamura M, Zhou P, Anrather J, Iadecola C. The neuroprotective effect of prostaglandin E2 EP1 receptor inhibition has a wide therapeutic window, is sustained in time and is not sexually dimorphic. J Cereb Blood Flow Metab. 2009; 29 (1):66–72.10.1038/jcbfm.2008.88 [PubMed: 18648380]

Ahmad AS, Maruyama T, Narumiya S, Doré S. PGE2 EP1 Receptor Deletion Attenuates 6-OHDA-Induced Parkinsonism in Mice: Old Switch, New Target. Neurotox Res. 2013; 23 (3):260–266.10.1007/s12640-013-9381-8 [PubMed: 23385625]

Ahmad AS, Saleem S, Ahmad M, Doré S. Prostaglandin EP1 receptor contributes to excitotoxicity and focal ischemic brain damage. Toxicol Sci. 2006; 89 (1):265–270.10.1093/toxsci/kfj022 [PubMed: 16237196]

Ahmad AS, Yun YT, Ahmad M, Maruyama T, Doré S. Selective blockade of PGE2 EP1 receptor protects brain against experimental ischemia and excitotoxicity, and hippocampal slice cultures against oxygen-glucose deprivation. Neurotox Res. 2008; 14 (4):343–351. [PubMed: 19073437]

Aronowski J, Hall CE. New horizons for primary intracerebral hemorrhage treatment: experience from preclinical studies. Neurol Res. 2005; 27 (3):268–279.10.1179/016164105X25225 [PubMed: 15845210]

Aronowski J, Zhao X. Molecular pathophysiology of cerebral hemorrhage: secondary brain injury. Stroke. 2011; 42 (6):1781–1786.10.1161/STROKEAHA.110.596718 [PubMed: 21527759]

Broderick JP, Adams HP Jr, Barsan W, Feinberg W, Feldmann E, Grotta J, Kase C, Krieger D, Mayberg M, Tilley B, Zabramski JM, Zuccarello M. Guidelines for the management of spontaneous intracerebral hemorrhage: A statement for healthcare professionals from a special writing group of the Stroke Council, American Heart Association. Stroke. 1999; 30 (4):905–915. [PubMed: 10187901]

Carlson NG, Rojas MA, Black JD, Redd JW, Hille J, Hill KE, Rose JW. Microglial inhibition of neuroprotection by antagonists of the EP1 prostaglandin E2 receptor. J Neuroinflammation. 2009; 6:5.10.1186/1742-2094-6-5 [PubMed: 19222857]

Chen L, Zhang X, Chen-Roetling J, Regan RF. Increased striatal injury and behavioral deficits after intracerebral hemorrhage in hemopexin knockout mice. J Neurosurg. 2011; 114 (4):1159–1167.10.3171/2010.10.JNS10861 [PubMed: 21128737]

Choi JS, Kim HY, Chun MH, Chung JW, Lee MY. Expression of prostaglandin E2 receptor subtypes, EP2 and EP4, in the rat hippocampus after cerebral ischemia and ischemic tolerance. Cell Tissue Res. 2006; 324 (2):203–211.10.1007/s00441-005-0121-0 [PubMed: 16437207]

Chu K, Jeong SW, Jung KH, Han SY, Lee ST, Kim M, Roh JK. Celecoxib induces functional recovery after intracerebral hemorrhage with reduction of brain edema and perihematomal cell death. J Cereb Blood Flow Metab. 2004; 24 (8):926–933.10.1097/01.WCB.0000130866.25040.7D [PubMed: 15362723]

Cimino PJ, Keene CD, Breyer RM, Montine KS, Montine TJ. Therapeutic targets in prostaglandin E2 signaling for neurologic disease. Curr Med Chem. 2008; 15 (19):1863–1869. [PubMed: 18691044]

Clark W, Gunion-Rinker L, Lessov N, Hazel K. Citicoline treatment for experimental intracerebral hemorrhage in mice. Stroke. 1998; 29 (10):2136–2140. [PubMed: 9756595]

Davis SM, Donnan GA. The stroke-prone state: rapid assessment of transient ischemic attacks. Stroke. 2006; 37 (4):1140. 01.STR.0000209245.05915.df. [PubMed: 16543514]

Doré S, Otsuka T, Mito T, Sugo N, Hand T, Wu L, Hurn PD, Traystman RJ, Andreasson K. Neuronal overexpression of cyclooxygenase-2 increases cerebral infarction. Ann Neurol. 2003; 54 (2):155–162.10.1002/ana.10612 [PubMed: 12891667]

Dunham NW, Miya TS. A note on a simple apparatus for detecting neurological deficit in rats and mice. J Am Pharm Assoc Am Pharm Assoc (Baltim). 1957; 46 (3):208–209. [PubMed: 13502156]

Funk CD, Furci L, FitzGerald GA, Grygorczyk R, Rochette C, Bayne MA, Abramovitz M, Adam M, Metters KM. Cloning and expression of a cDNA for the human prostaglandin E receptor EP1 subtype. J Biol Chem. 1993; 268 (35):26767–26772. [PubMed: 8253813]

Giulian D, Chen J, Ingeman JE, George JK, Noponen M. The role of mononuclear phagocytes in wound healing after traumatic injury to adult mammalian brain. J Neurosci. 1989; 9 (12):4416–4429. [PubMed: 2480402]

Go AS, Mozaffarian D, Roger VL, Benjamin EJ, Berry JD, Borden WB, Bravata DM, Dai S, Ford ES, Fox CS, Franco S, Fullerton HJ, Gillespie C, Hailpern SM, Heit JA, Howard VJ, Huffman MD, Kissela BM, Kittner SJ, Lackland DT, Lichtman JH, Lisabeth LD, Magid D, Marcus GM, Marelli A, Matchar DB, McGuire DK, Mohler ER, Moy CS, Mussolino ME, Nichol G, Paynter NP, Schreiner PJ, Sorlie PD, Stein J, Turan TN, Virani SS, Wong ND, Woo D, Turner MB. Heart disease and stroke statistics--2013 update: a report from the American Heart Association. Circulation. 2013; 127 (1):e6–e245.10.1161/CIR.0b013e31828124ad [PubMed: 23239837]

Gu Y, Hua Y, Keep RF, Morgenstern LB, Xi G. Deferoxamine reduces intracerebral hematoma-induced iron accumulation and neuronal death in piglets. Stroke. 2009; 40 (6):2241–2243.10.1161/STROKEAHA.108.539536 [PubMed: 19372448]

Hebert RL, Jacobson HR, Breyer MD. PGE2 inhibits AVP-induced water flow in cortical collecting ducts by protein kinase C activation. Am J Physiol. 1990; 259 (2 Pt 2):F318–325. [PubMed: 2167017]

Hoffmann PR, Kench JA, Vondracek A, Kruk E, Daleke DL, Jordan M, Marrack P, Henson PM, Fadok VA. Interaction between phosphatidylserine and the phosphatidylserine receptor inhibits immune responses in vivo. J Immunol. 2005; 174 (3):1393–1404. 174/3/1393. [PubMed: 15661897]

Huynh ML, Fadok VA, Henson PM. Phosphatidylserine-dependent ingestion of apoptotic cells promotes TGF-beta1 secretion and the resolution of inflammation. J Clin Invest. 2002; 109 (1):41–50.10.1172/JCI11638 [PubMed: 11781349]

Ito D, Tanaka K, Suzuki S, Dembo T, Fukuuchi Y. Enhanced expression of Iba1, ionized calcium-binding adapter molecule 1, after transient focal cerebral ischemia in rat brain. Stroke. 2001; 32 (5):1208–1215. [PubMed: 11340235]

James ML, Wang H, Venkatraman T, Song P, Lascola CD, Laskowitz DT. Brain natriuretic peptide improves long-term functional recovery after acute CNS injury in mice. J Neurotrauma. 2010; 27 (1):217–228.10.1089/neu.2009.1022 [PubMed: 19803787]

Jones BJ, Roberts DJ. The quantiative measurement of motor inco-ordination in naive mice using an acelerating rotarod. J Pharm Pharmacol. 1968; 20 (4):302–304. [PubMed: 4384609]

Kawano T, Anrather J, Zhou P, Park L, Wang G, Frys KA, Kunz A, Cho S, Orio M, Iadecola C. Prostaglandin E2 EP1 receptors: downstream effectors of COX-2 neurotoxicity. Nat Med. 2006; 12 (2):225–229. nm1362. [PubMed: 16432513]

Keep RF, Hua Y, Xi G. Intracerebral haemorrhage: mechanisms of injury and therapeutic targets. Lancet Neurol. 2012; 11 (8):720–731.10.1016/S1474-4422(12)701047 [PubMed: 22698888]

Keep RF, Xi G, Hua Y, Hoff JT. The deleterious or beneficial effects of different agents in intracerebral hemorrhage: think big, think small, or is hematoma size important? Stroke. 2005; 36 (7):1594–1596. 01.STR.0000170701.41507.e1. [PubMed: 15933250]

Koizumi S, Shigemoto-Mogami Y, Nasu-Tada K, Shinozaki Y, Ohsawa K, Tsuda M, Joshi BV, Jacobson KA, Kohsaka S, Inoue K. UDP acting at P2Y6 receptors is a mediator of microglial phagocytosis. Nature. 2007; 446 (7139):1091–1095. nature05704. [PubMed: 17410128]

Komotar RJ, Kim GH, Sughrue ME, Otten ML, Rynkowski MA, Kellner CP, Hahn DK, Merkow MB, Garrett MC, Starke RM, Connolly ES. Neurologic assessment of somatosensory dysfunction following an experimental rodent model of cerebral ischemia. Nat Protoc. 2007; 2 (10):2345–2347. nprot.2007.359. [PubMed: 17947976]

MacLellan CL, Silasi G, Poon CC, Edmundson CL, Buist R, Peeling J, Colbourne F. Intracerebral hemorrhage models in rat: comparing collagenase to blood infusion. J Cereb Blood Flow Metab. 2008; 28 (3):516–525. 9600548. [PubMed: 17726491]

Matsushita K, Meng W, Wang X, Asahi M, Asahi K, Moskowitz MA, Lo EH. Evidence for apoptosis after intercerebral hemorrhage in rat striatum. J Cereb Blood Flow Metab. 2000; 20 (2):396–404.10.1097/00004647-200002000-00022 [PubMed: 10698078]

Nguyen VT, Benveniste EN. Critical role of tumor necrosis factor-alpha and NF-kappa B in interferon-gamma -induced CD40 expression in microglia/macrophages. J Biol Chem. 2002; 277 (16): 13796–13803.10.1074/jbc.M111906200 [PubMed: 11830590]

Phillis JW, Horrocks LA, Farooqui AA. Cyclooxygenases, lipoxygenases, and epoxygenases in CNS: their role and involvement in neurological disorders. Brain Res Rev. 2006; 52 (2):201–243. S0165-0173(06)00011-7. [PubMed: 16647138]

Qureshi AI, Tuhrim S, Broderick JP, Batjer HH, Hondo H, Hanley DF. Spontaneous intracerebral hemorrhage. N Engl J Med. 2001; 344 (19):1450–1460.10.1056/NEJM200105103441907 [PubMed: 11346811]

Regan RF, Panter SS. Neurotoxicity of hemoglobin in cortical cell culture. Neurosci Lett. 1993; 153 (2):219–222. [PubMed: 8327197]

Ribo M, Grotta JC. Latest advances in intracerebral hemorrhage. Curr Neurol Neurosci Rep. 2006; 6 (1):17–22. [PubMed: 16469266]

Saleem S, Li RC, Wei G, Doré S. Effects of EP1 receptor on cerebral blood flow in the middle cerebral artery occlusion model of stroke in mice. J Neurosci Res. 2007; 85 (11):2433–2440.10.1002/jnr.21399 [PubMed: 17600836]

Schallert T, Fleming SM, Leasure JL, Tillerson JL, Bland ST. CNS plasticity and assessment of forelimb sensorimotor outcome in unilateral rat models of stroke, cortical ablation, parkinsonism and spinal cord injury. Neuropharmacology. 2000; 39 (5):777–787. S0028390800000058. [PubMed: 10699444]

Schmued LC, Hopkins KJ. Fluoro-Jade B: a high affinity fluorescent marker for the localization of neuronal degeneration. Brain Res. 2000; 874 (2):123–130. S0006-8993(00)02513-0. [PubMed: 10960596]

Shah ZA, Nada SE, Dore S. Heme oxygenase 1, beneficial role in permanent ischemic stroke and in Gingko biloba (EGb 761) neuroprotection. Neuroscience. 2011; 180:248–255.10.1016/j.neuroscience.2011.02.031 [PubMed: 21334424]

Simmer JP, Hu Y, Lertlam R, Yamakoshi Y, Hu JC. Hypomaturation enamel defects in Klk4 knockout/LacZ knockin mice. J Biol Chem. 2009; 284 (28):19110–19121.10.1074/jbc.M109.013623 [PubMed: 19578120]

Smirkin A, Matsumoto H, Takahashi H, Inoue A, Tagawa M, Ohue S, Watanabe H, Yano H, Kumon Y, Ohnishi T, Tanaka J. Iba1(+)/NG2(+) macrophage-like cells expressing a variety of neuroprotective factors ameliorate ischemic damage of the brain. J Cereb Blood Flow Metab. 2010; 30 (3):603–615.10.1038/jcbfm.2009.233 [PubMed: 19861972]

Takahashi K, Prinz M, Stagi M, Chechneva O, Neumann H. TREM2-transduced myeloid precursors mediate nervous tissue debris clearance and facilitate recovery in an animal model of multiple sclerosis. PLoS Med. 2007; 4 (4):e124. 06-PLME-RA-0690R2. [PubMed: 17425404]

Takahashi K, Rochford CD, Neumann H. Clearance of apoptotic neurons without inflammation by microglial triggering receptor expressed on myeloid cells-2. J Exp Med. 2005; 201 (4):647–657. jem.20041611. [PubMed: 15728241]

Tang ZP, Xie XW, Shi YH, Liu N, Zhu SQ, Li ZW, Chen Y. Combined transplantation of neural stem cells and olfactory ensheathing cells improves the motor function of rats with intracerebral hemorrhage. Biomed Environ Sci. 2010; 23 (1):62–67. [PubMed: 20486438]

Tikka TM, Koistinaho JE. Minocycline provides neuroprotection against N-methyl-D-aspartate neurotoxicity by inhibiting microglia. J Immunol. 2001; 166 (12):7527–7533. [PubMed: 11390507]

Wang J, Doré S. Heme oxygenase-1 exacerbates early brain injury after intracerebral haemorrhage. Brain. 2007a; 130 (Pt 6):1643–1652. 130/6/1643. [PubMed: 17525142]

Wang J, Doré S. Inflammation after intracerebral hemorrhage. J Cereb Blood Flow Metab. 2007b; 27 (5):894–908. 9600403. [PubMed: 17033693]

Wang J, Fields J, Zhao C, Langer J, Thimmulappa RK, Kensler TW, Yamamoto M, Biswal S, Doré S. Role of Nrf2 in protection against intracerebral hemorrhage injury in mice. Free Radic Biol Med. 2007; 43 (3):408–414. S0891-5849(07)00287-0. [PubMed: 17602956]

Wang J, Zhuang H, Doré S. Heme oxygenase 2 is neuroprotective against intracerebral hemorrhage. Neurobiol Dis. 2006; 22 (3):473–476. S0969-9961(05)00343-8. [PubMed: 16459095]

Wasserman JK, Schlichter LC. Neuron death and inflammation in a rat model of intracerebral hemorrhage: effects of delayed minocycline treatment. Brain Res. 2007; 1136 (1):208–218. S0006-8993(06)03576-1. [PubMed: 17223087]

Watabe A, Sugimoto Y, Honda A, Irie A, Namba T, Negishi M, Ito S, Narumiya S, Ichikawa A. Cloning and expression of cDNA for a mouse EP1 subtype of prostaglandin E receptor. J Biol Chem. 1993; 268 (27):20175–20178. [PubMed: 7690750]

Wu G, Xi G, Huang F. Spontaneous intracerebral hemorrhage in humans: hematoma enlargement, clot lysis, and brain edema. Acta Neurochir Suppl. 2006; 96:78–80. [PubMed: 16671430]

Xue M, Del Bigio MR. Intracerebral injection of autologous whole blood in rats: time course of inflammation and cell death. Neurosci Lett. 2000; 283 (3):230–232. S030439400000971X. [PubMed: 10754230]

Yang SX, Wang YR, Qian C, He C. Neuron regeneration in aged rats after intracerebral hemorrhage. Zhejiang Da Xue Xue Bao Yi Xue Ban. 2008; 37 (4):386–392. [PubMed: 18705012]

Yrjanheikki J, Tikka T, Keinanen R, Goldsteins G, Chan PH, Koistinaho J. A tetracycline derivative, minocycline, reduces inflammation and protects against focal cerebral ischemia with a wide therapeutic window. Proc Natl Acad Sci U S A. 1999; 96 (23):13496–13500. [PubMed: 10557349]

Zhao X, Grotta J, Gonzales N, Aronowski J. Hematoma resolution as a therapeutic target: the role of microglia/macrophages. Stroke. 2009; 40 (3 Suppl):S92–94.10.1161/STROKEAHA.108.533158 [PubMed: 19064796]

Zhao X, Sun G, Zhang J, Strong R, Song W, Gonzales N, Grotta JC, Aronowski J. Hematoma resolution as a target for intracerebral hemorrhage treatment: role for peroxisome proliferator-activated receptor gamma in microglia/macrophages. Ann Neurol. 2007; 61 (4):352–362.10.1002/ana.21097 [PubMed: 17457822]

Zhou P, Qian L, Chou T, Iadecola C. Neuroprotection by PGE2 receptor EP1 inhibition involves the PTEN/AKT pathway. Neurobiol Dis. 2008; 29 (3):543–551.10.1016/j.nbd.2007.11.010 [PubMed: 18178094]

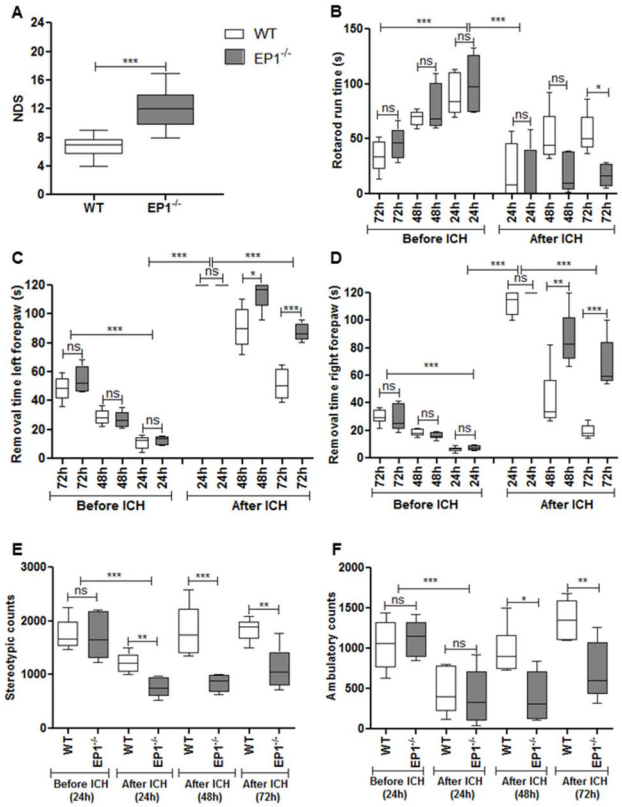

Fig 1.

EP1 deletion deteriorates neurological and functional outcome following collagenase-induced intracerebral hemorrhage (ICH) in mice. *(A)* Neurological deficit scoring showed that EP1$^{-/-}$ have significantly higher functional disability compared to wildtype (WT) mice at 72 h of ICH (P<0.0001). *(B)* Rotarod pre-training of WT and EP1$^{-/-}$ mice showed significant improvement of motor coordination on the accelerating rotarod with time (72 h vs. 24 h; P<0. 001). We did not find any significant difference between the two genotypes at any stage of pre-training. ICH injury leads to significant deficit in motor coordination following 24 h post hemorrhagic injury (P<0.001) for both genotypes. However, WT mice showed significant improvement in motor coordination on rotarod performance task compared to EP1$^{-/-}$ mice at 72 h post ICH (P<0.05). *(C & D)* Adhesive removal pre-training of WT and EP1$^{-/-}$ mice significantly shortened the time to remove tapes from both forepaws (72 vs. 24 h; P<0.001). No significant difference was found in both genotypes during any time of pre-training. ICH induces significant impairments in the ability to remove adhesive tape from their forepaws following 24 h of injury (P<0.001). WT mice recovered faster compared to EP1$^{-/-}$ mice and took significantly less time to remove tapes from both forepaws 72 h after ICH injury (P<0.001). *(E & F)* Open field activity did not show any significant difference in WT and EP1$^{-/-}$ mice before ICH. ICH injury induced significant impairment in both stereotypic *(E)* and ambulatory *(F)* activities (P<0.001). Following 72 h ICH injury, WT mice showed significant improvement in both kinds of activities compared to EP1$^{-/-}$ mice (P<0.05). Values are expressed as mean ± S.D of n=6 animals.

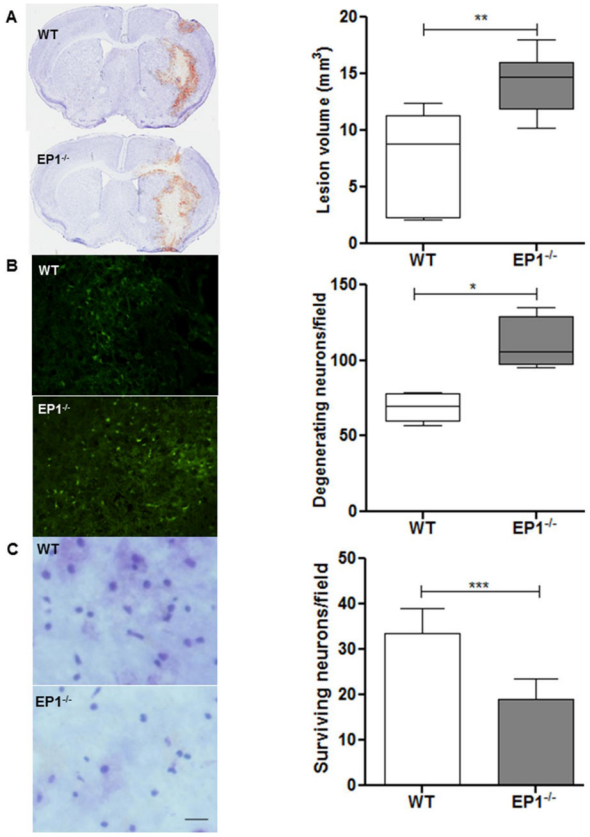

Fig 2.

Deletion of EP1 receptor increases brain injury volume, cell death, and reduced cell survival. *(A)* Representative photomicrograph showing brain sections from EP1$^{-/-}$ and WT mice subjected to ICH injury. Quantification showed significantly larger brain injury volume in EP1$^{-/-}$ compared to WT mice at 72 h after ICH injury (P<0.01; n=6). *(B)* Fluoro-Jade B staining photomicrograph and quantification showed a significant increase in degenerating neurons in EP1$^{-/-}$ compared to WT mice following 72 h ICH (P<0.02; n = 4). *(C)* Representative image and quantitative analysis of the surviving neurons with Cresyl Violet staining showed significantly more surviving neurons in the peri-hematoma region of WT compared to the EP1$^{-/-}$ mice at 72 h post ICH (P<0.001; n=4). Values are expressed as mean ± S.D.

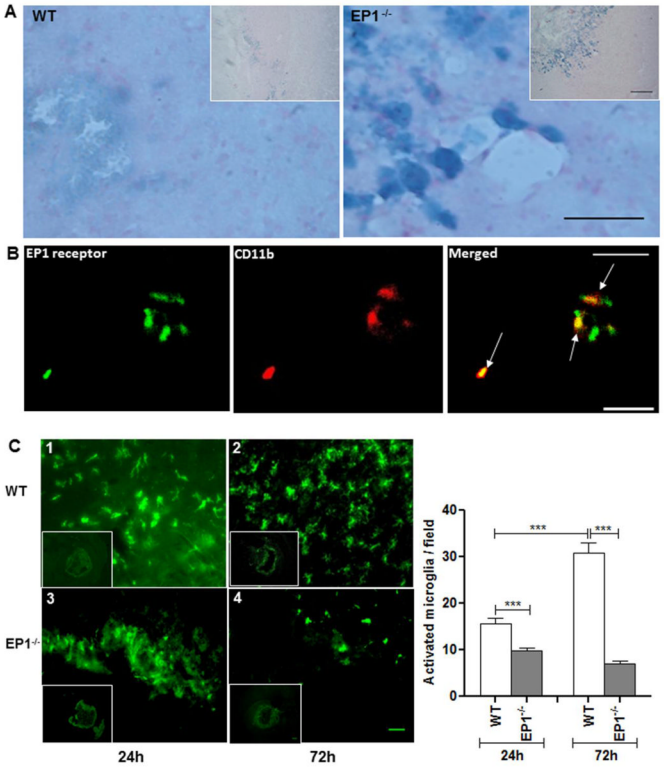

Fig 3.

Expression of EP1 receptor and cellular localization of microglia after induction of ICH. *(A)* X-gal staining showed significantly higher β-galactosidase activity in microglia-like cells in the peri-hematoma areas of $EP1^{-/-}$ mice at 72 h, whereas WT mice had weak β-galactosidase activity. Inset shows β-galactosidase-positive cells at lower magnification. *(B)* Double immunofluorescence staining for immune-reactive EP1 receptor (green) and CD11b (cell marker for microglia/macrophages; red), which were visualized by Cy3-conjugated secondary antibodies. Arrows point to areas of co-localization in brain section obtained at 72 h after ICH (n=4). *(C)* Effect of EP1 receptor deletion on microglial activation after induced intracerebral hematoma. The distribution and morphology of microglia (Iba1-positive) are shown in coronal sections collected at 24 and 72 h from WT (1, 2) and $EP1^{-/-}$ (3, 4) mice, respectively. Activated microglia (with large cell bodies and thick, short processes) were mainly observed in the peri-hematoma region in both groups and the quantification showed that the $EP1^{-/-}$ mice had significantly fewer activated microglia than the WT mice at 24 and 72 h ($P<0.001$; n=4). Moreover, the number of activated microglia increased markedly in WT mice from 24 to 72 h, however there was no significant change observed in microglia in $EP1^{-/-}$ mice, at 24 and 72 h post ICH injury (n=4). Values are expressed as mean ± S.D.

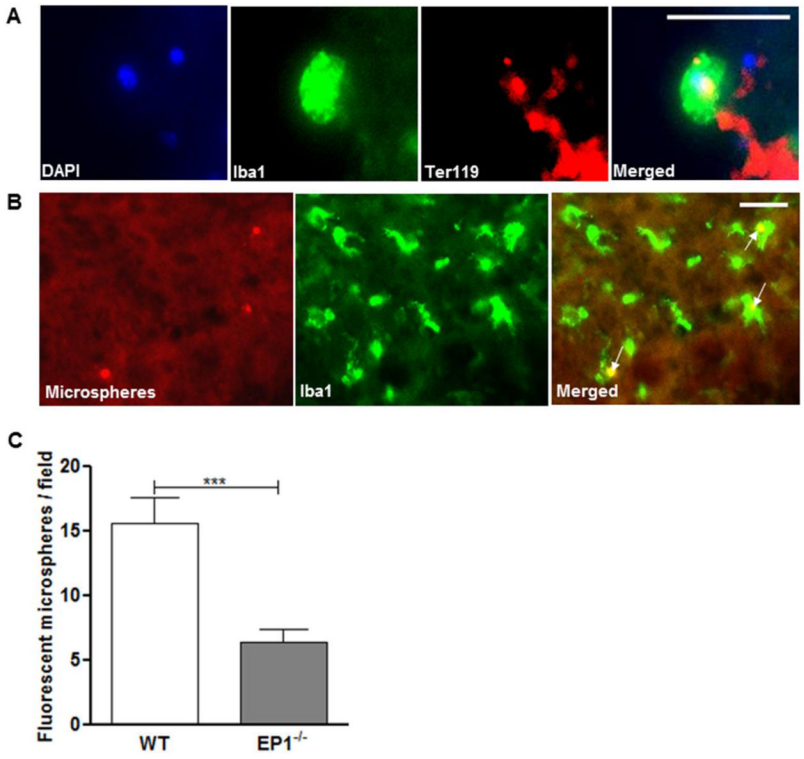

Fig 4.

Effect of EP1 receptor deletion on microglial phagocytosis after induced intracerebral hematoma. *(A)* Representative pictures of red blood cells (red, anti-Ter119) phagocytosed by microglia (green, anti-Iba1) in the peri-hematoma regions *in vivo*. Cell nuclei are shown by DAPI-staining (blue). *(B)* Images of fluorescent microspheres (red) attached to or taken up by microglia (green, anti-Iba1) *in vivo*. Arrows point to areas of co-localization. *(C)* Quantitative analysis of phagocytosis *in vivo*. $EP1^{-/-}$ mice had significantly fewer colocalized fluorescent microspheres with microglia than the WT mice 72 h ($P<0.001$; n=4). Values are expressed as mean ± S.D.